USING STAINLESS STEEL STRATEGICALLY IN KEY LOCATIONS OF STEEL FRAMED BUILDINGS FOR IMPROVED FIRE AND POST-FIRE PERFORMANCE

Hadi EL SAMAD, **Luke LAPIRA** and Katherine A. CASHELL

Department of Civil, Environmental and Geomatic Engineering,
University College London, UCL, UK

Emails: hadi.samad.22@ucl.ac.uk, l.lapira@ucl.ac.uk, k.cashell@ucl.ac.uk,

Background and motivation

- Critical need to brace the built environment for extreme conditions.
- The aim is to achieve this goal using high-performance materials.
  - Such as stainless steel.

Steel after building fire

RESIST Project

EPSRC funded research project

Vision

To bring a step-change in resilience of new and rehabilitated steel buildings by the strategic use of highly ductile elements in key locations such as the joints

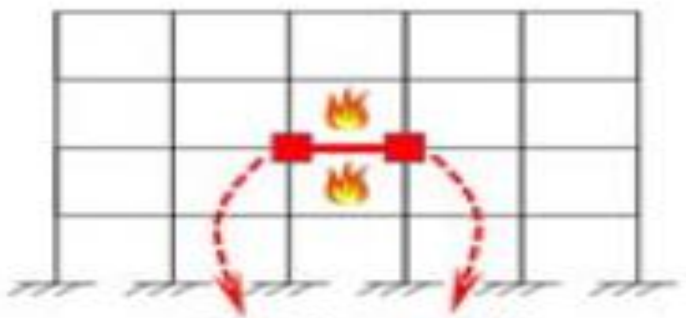

Aim

Replacing carbon steel components in the joint zone with stainless steel.

Why stainless steel?

- Carbon steel has a ductility of approximately 20-30%
- Stainless steel has a ductility of approximately 40-60%
- Stainless steel also boasts improved:
  - Corrosion resistance.
  - Durability.
  - Elevated temperature behavior.

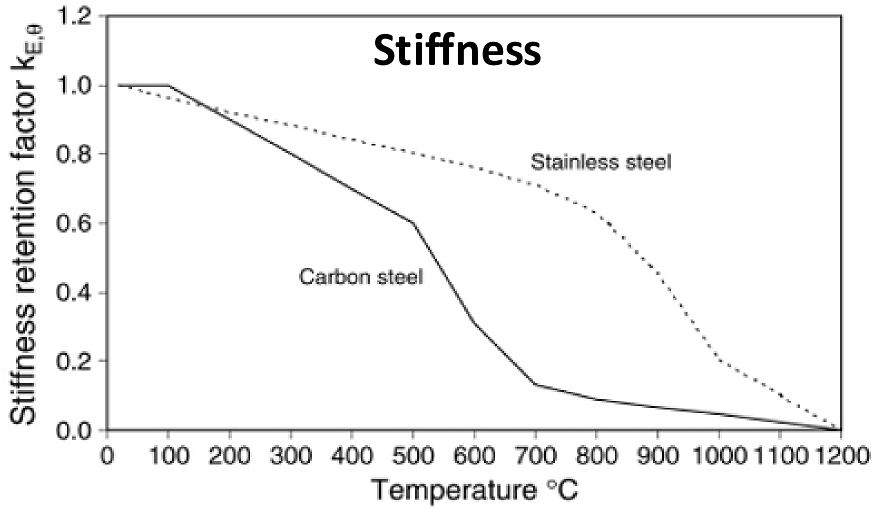

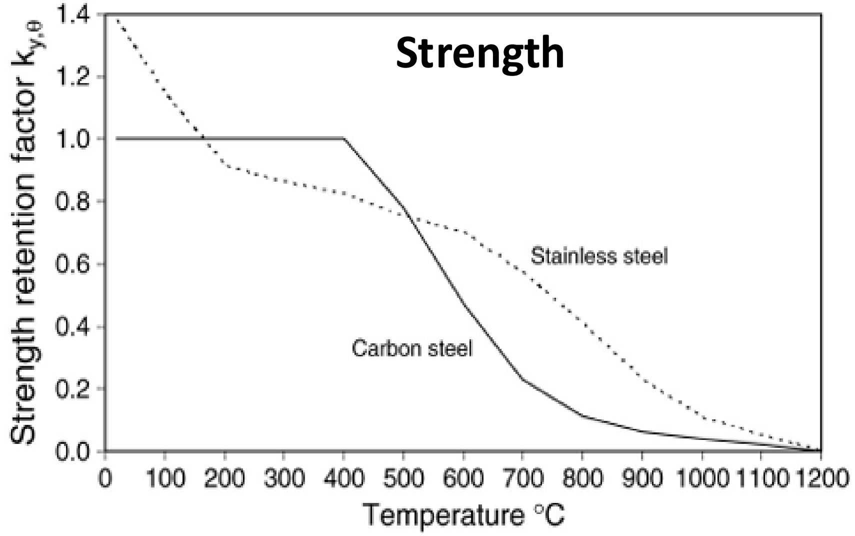

Figure 1: Comparison of stiffness and strength reduction of carbon steel and Stainless steel with elevated temperature [1]

RESIST Project - EPSRC

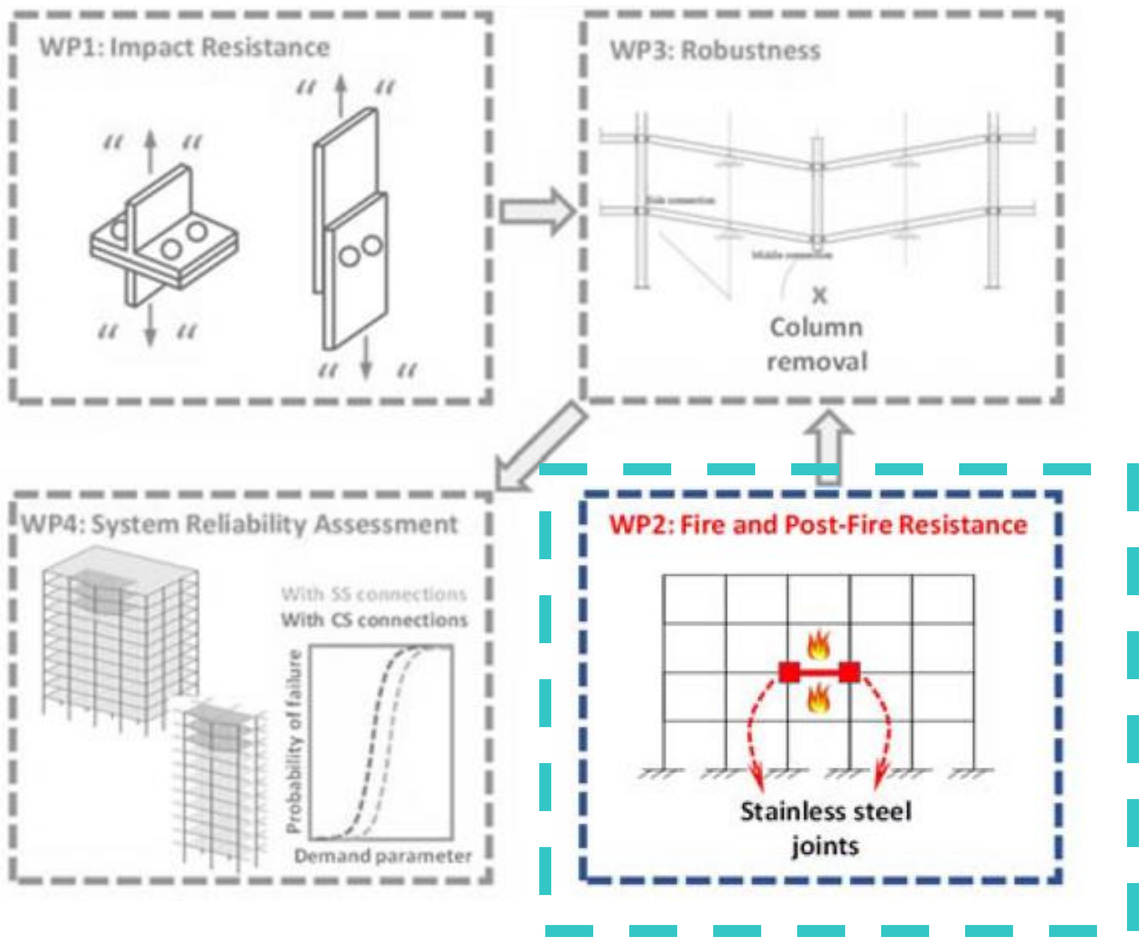

Research objectives of the RESIST Project

1. Experimentally and numerically investigate stainless steel joints under extreme loads, including high strain rates and elevated temperatures.
2. Develop component-based models for joints under various loading conditions.
3. Demonstrate effectiveness of strategic use of stainless steel in key joint locations.
4. Develop framework and recommendations for designing resilient buildings using hybrid stainless steel joints.
5. Disseminate findings to practicing engineers, researchers and code drafting committees.

Hadi's (current) research objectives

1. Provide new test data for mechanical properties of H500 after exposure to fire.

- H500 is a new grade of austenitic stainless steel developed by Outokumpu [2].
- Focus on failure modes of specimens after exposure to different temperatures.

2. Development of a finite element (FE) model for analysing structural *fire* and *post-fire* response of semi-rigid flush endplate connection.

- FE model validation with published experimental results.

3. Parametric study

- Parametric study replacing:
  - Endplate material with post-fire H500 properties (obtained experimentally).
  - Bolt & endplate materials with various stainless steel grades during fire.

1. Post-fire experimental study

Specimen, test device and procedure

- **Total of 46 coupon specimens were heated in an electrical furnace.**
  - Specimens were heated from ambient temperature at a rate of **10 °C/min.**
  - Exposed to the target temperature for **20 minutes.**
- **Two cooling techniques were used**
  - Cool in **water** (CIW) in a metal bucket.
  - Cool in **air** on top of a brick.

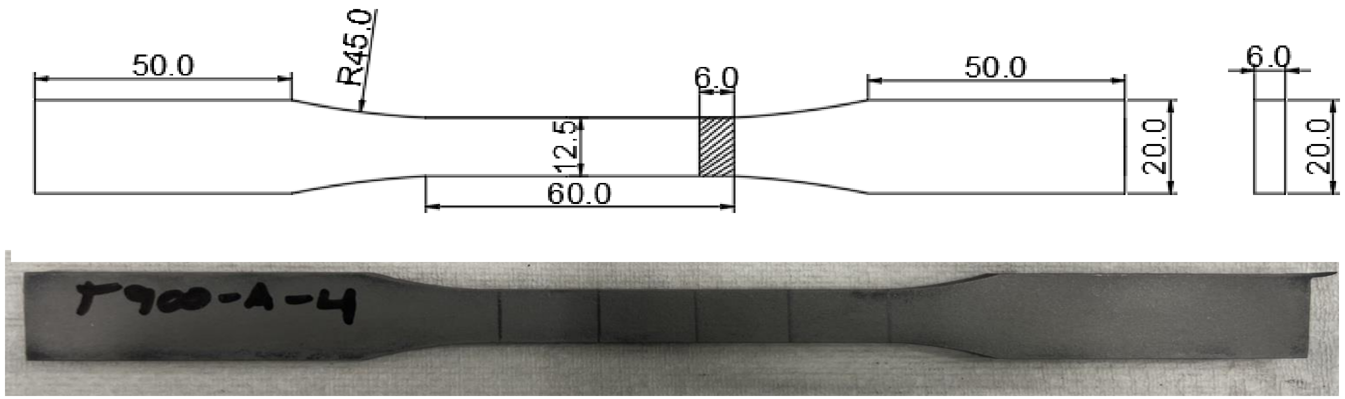

Coupon specimen

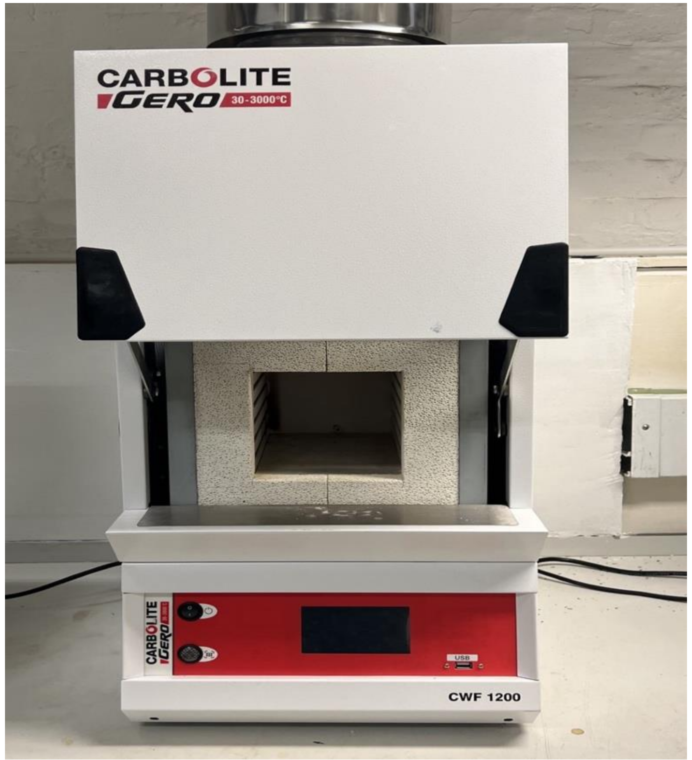

Carbolite furnace

Tensile testing

- Tensile tests conducted at ambient temperature using Zwick/Roell UTM to BS EN ISO 6892-1
- DIC to measure surface strain field; capturing images at 1 Hz.
- Random speckle paint pattern was applied to the surface.
- Strains were processed using a virtual strain gauge.

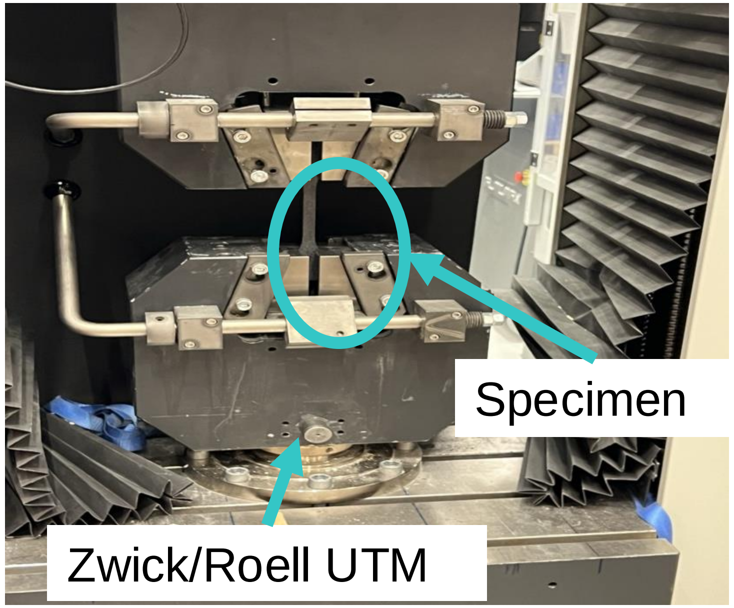

Zwick/Roell

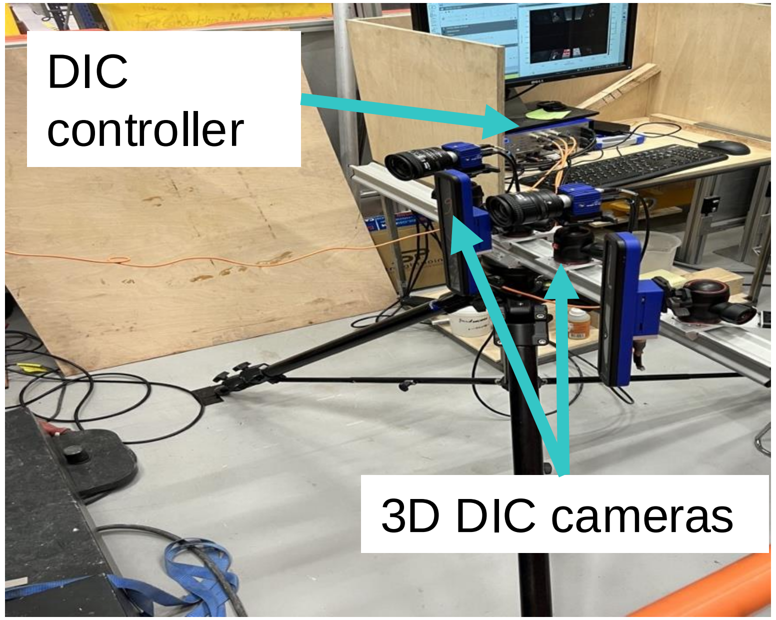

DIC

Speckle pattern

Figure 2: Test set-up and specimen preparation

Post-fire stress-strain curves for H500 CIW

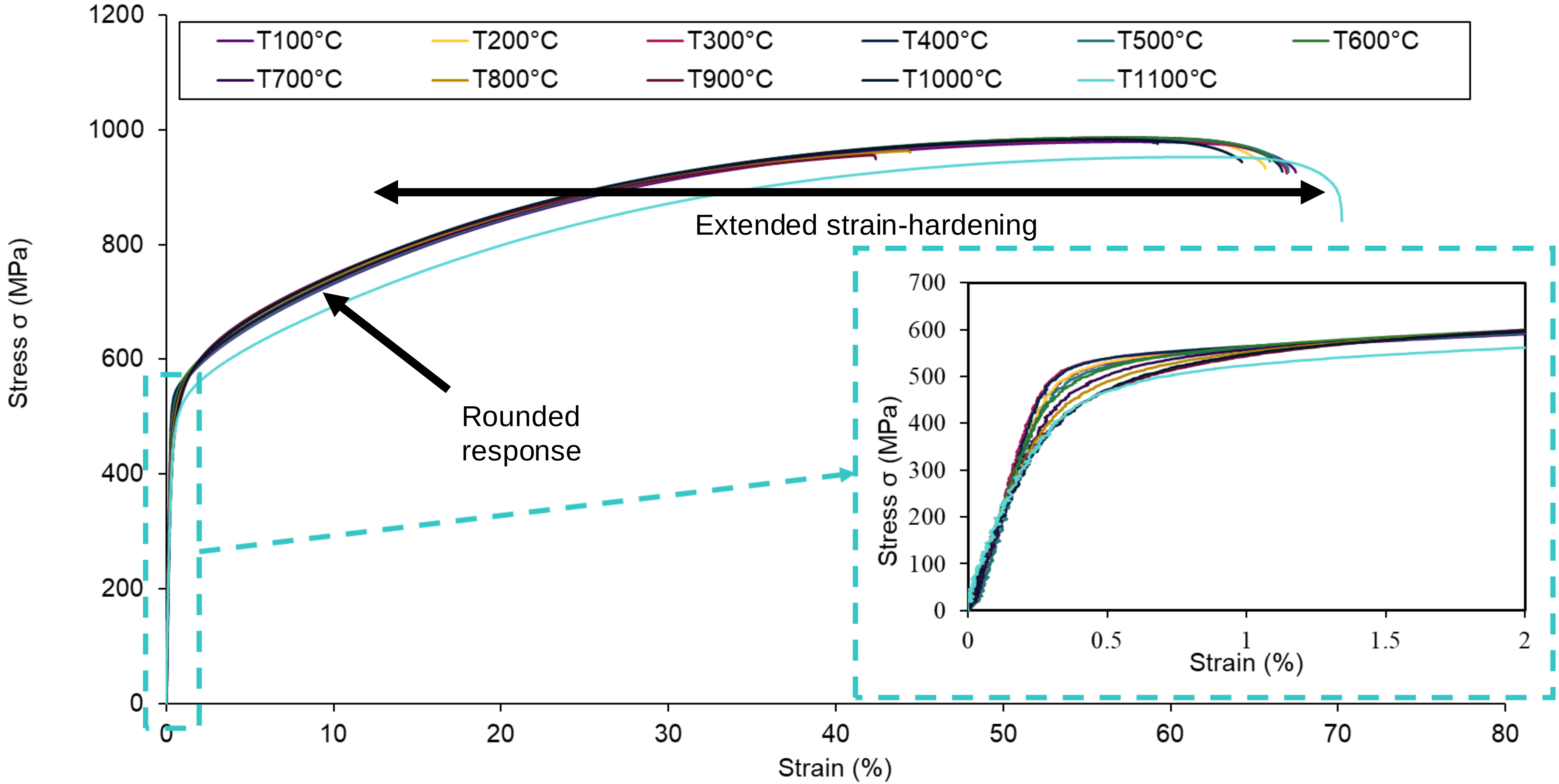

Figure 3: Post-fire stress-strain curve cooled in water (CIW)

Post-fire mechanical properties of H500

UCL

Table 1: Mechanical properties

Temperature θ (°C)	E_θ (MPa)	$f_{0.2p,\theta}$ (MPa)	$f_{1.0p,\theta}$ (MPa)	$f_{1.5p,\theta}$ (MPa)	$f_{2p,\theta}$ (MPa)	$f_{u,\theta}$ (MPa)	$\varepsilon_{u,\theta}$ (%)	$\varepsilon_{f,\theta}$ (%)
20	194764	525	570.3	585.6	600	979.1	57.2	65.1
100	203239	524.1	568.4	584.5	598.6	979.2	57.4	67.5
200	199021	524.8	572.5	588.5	603.3	986.4	57.4	65.7
300	198709	534.4	573.2	586.6	600.5	982.1	56.6	66.9
400	196403	539.6	574.3	591	604	986.6	57.6	66.7
500	177337	521.2	572.8	588.2	601.6	984.4	57.6	67
600	176701	517.6	578.6	594.8	608.3	986.2	56.7	65.9
700	157387	503.7	574.5	591	605.6	983.6	55.9	59.2
800	160330	492.2	573.6	593.5	610	963.1	44.2	44.5
900	151860	475.7	567.5	595.5	613.8	955.8	42.1	42.4
1000	148272	482.1	573.3	594.6	610.2	983.3	56.1	64.3
1100	135433	475.6	541.4	559.9	572.6	952.7	61.2	70.2

Stiffness regained (20–400 °C)

Stiffness loss (500–1100 °C)

Failure modes

Ductile failure with necking

T = [20 – 600 °C],

T = [1000-1100 °C]

Necking

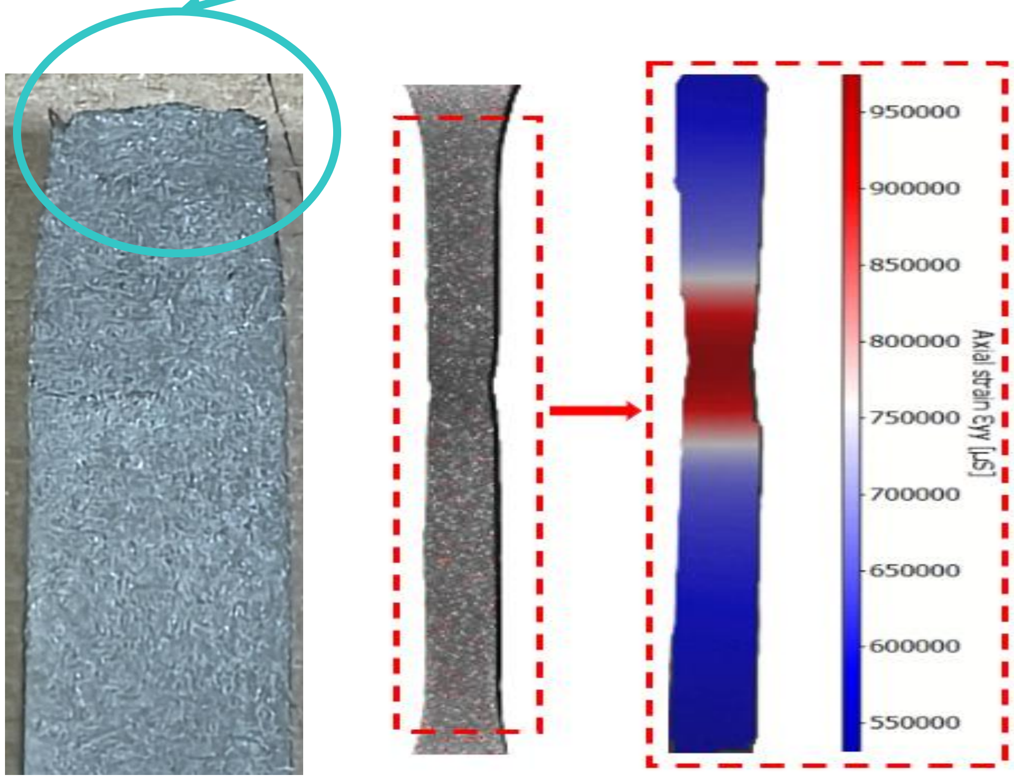

400 °C

Sudden brittle failure

T = [700 – 900 °C]

No signs of necking

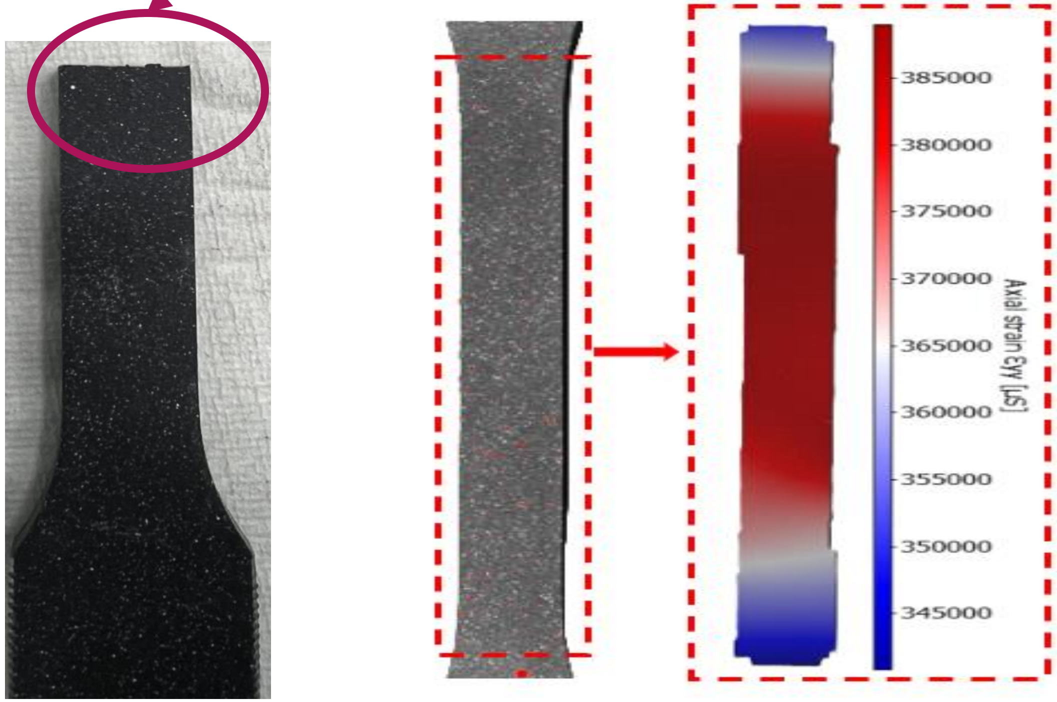

900 °C

2. Finite element (FE) analysis

FE Model assembly

- Geometric details modelled identically to experiments published in [3].
  - Symmetrical, so half of the connection is modelled.

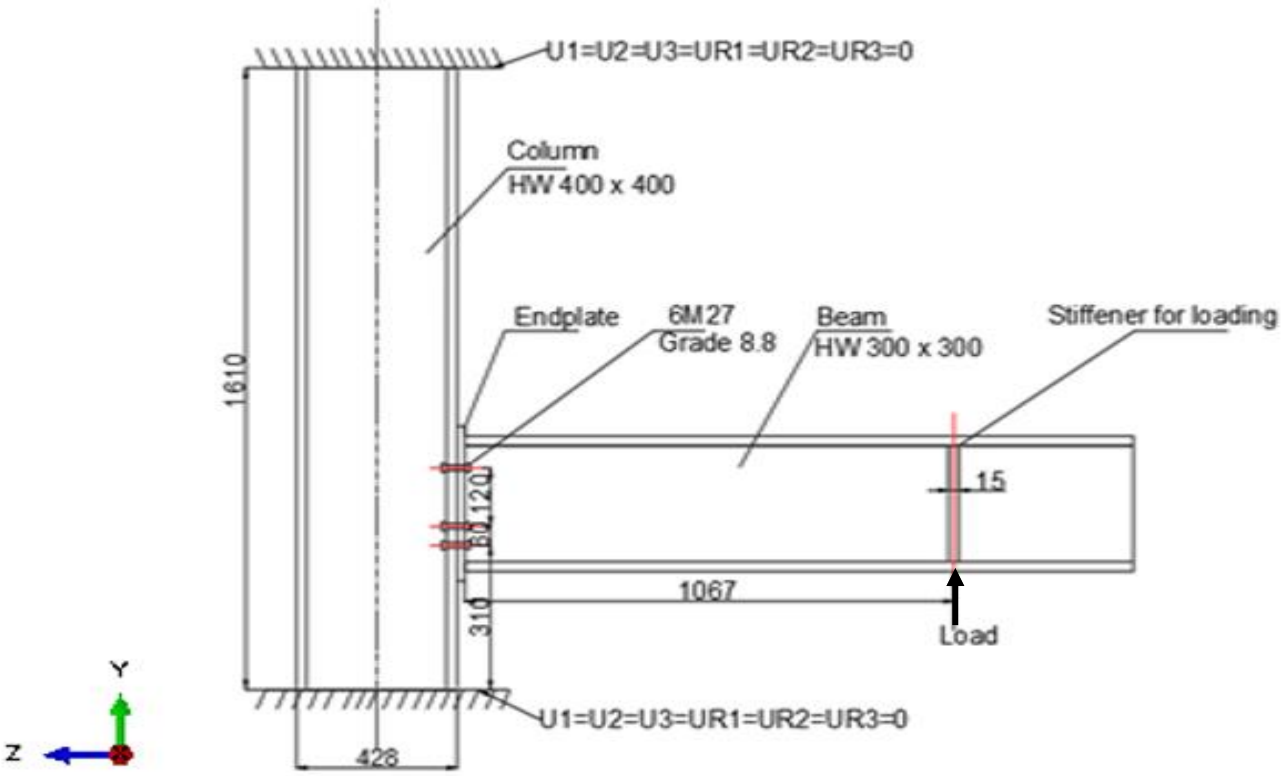

Figure 4: Full connection

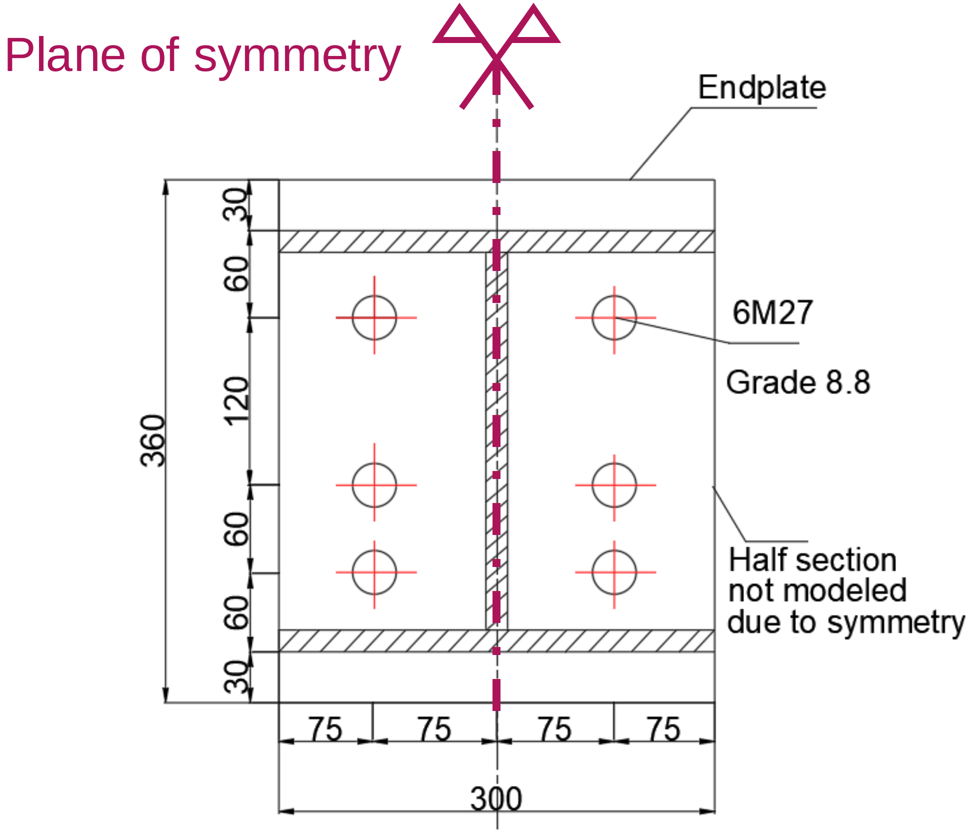

Figure 5: Endplate

FE Meshing and Interactions

- Mesh elements: **C3D8I**
  - Bolts = 3 mm
  - Columns = 9 mm
  - Beams = 5.5 mm
  - Endplate = 8 mm
- Static loading accounting for material and geometric nonlinearity (GMNA)
- Contact friction coefficient **0.44**
- Elevated temperature study:
  - Temperature field set to 550 °C

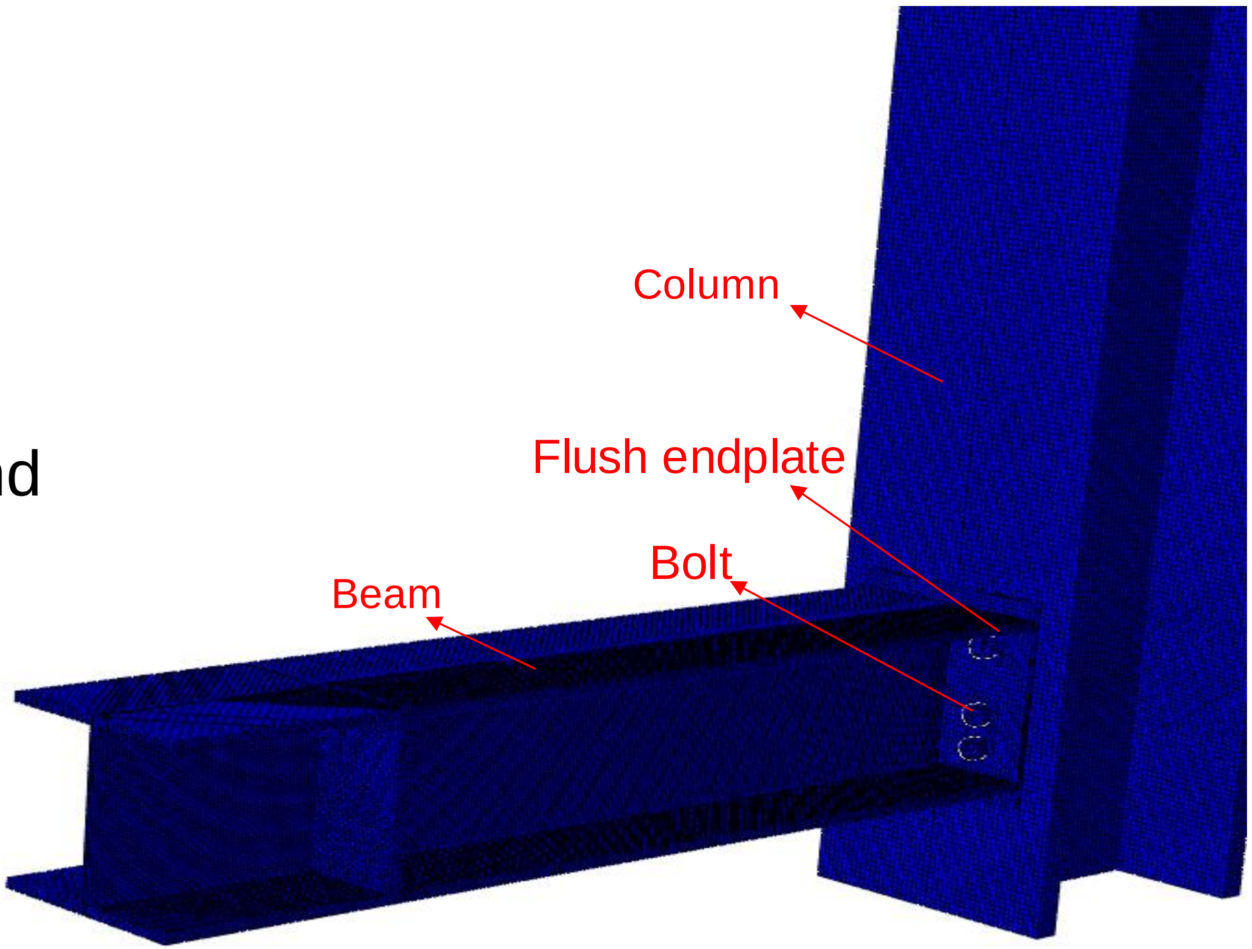

Abaqus 3D model

FE Material properties

Material properties tested in [3]:

• Column and Beam:	Q345
• Bolts:	Grade 8.8
• End plate:	S690, S960

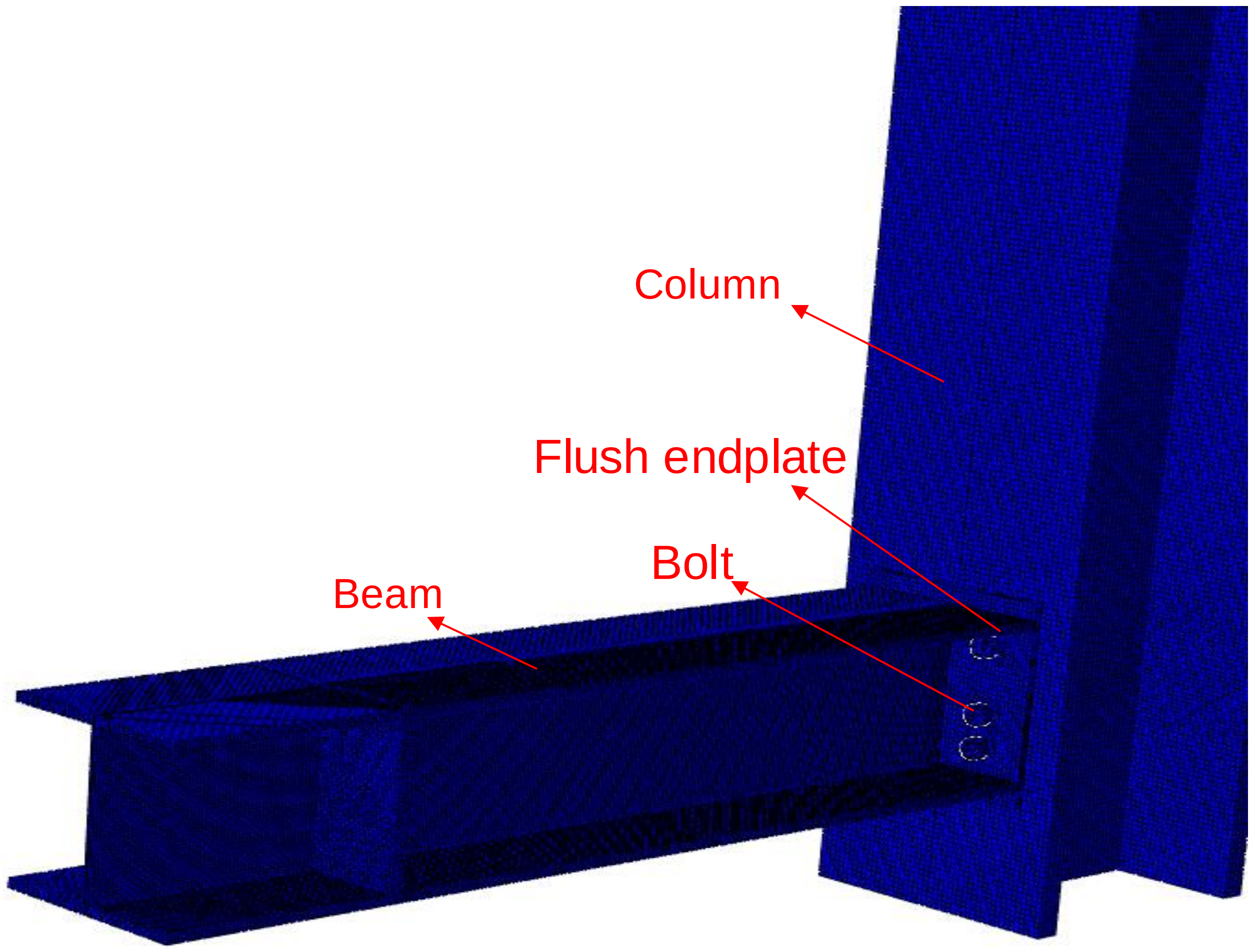

Abaqus 3D model

FE Material properties

- Ambient and post-fire material properties are identical to [3].
- Post-fire of beam and column are 90% of ambient [4].

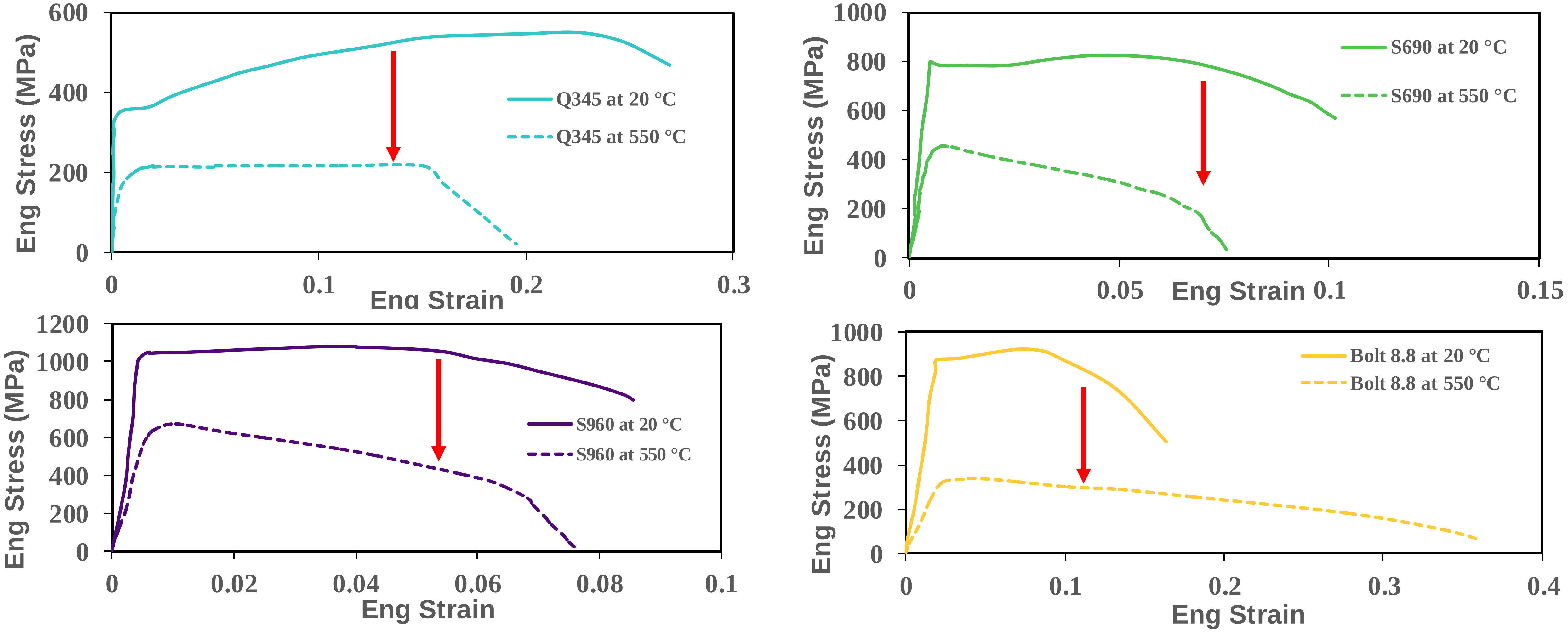

Figure 6: Ambient and elevated temperature material stress-strain curves

Validation of FE Model

Ambient temperature validation

- Connection Type 1: Endplate material S690 with 15 mm thickness.
- Connection Type 2: Endplate material S960 with 12 mm thickness.

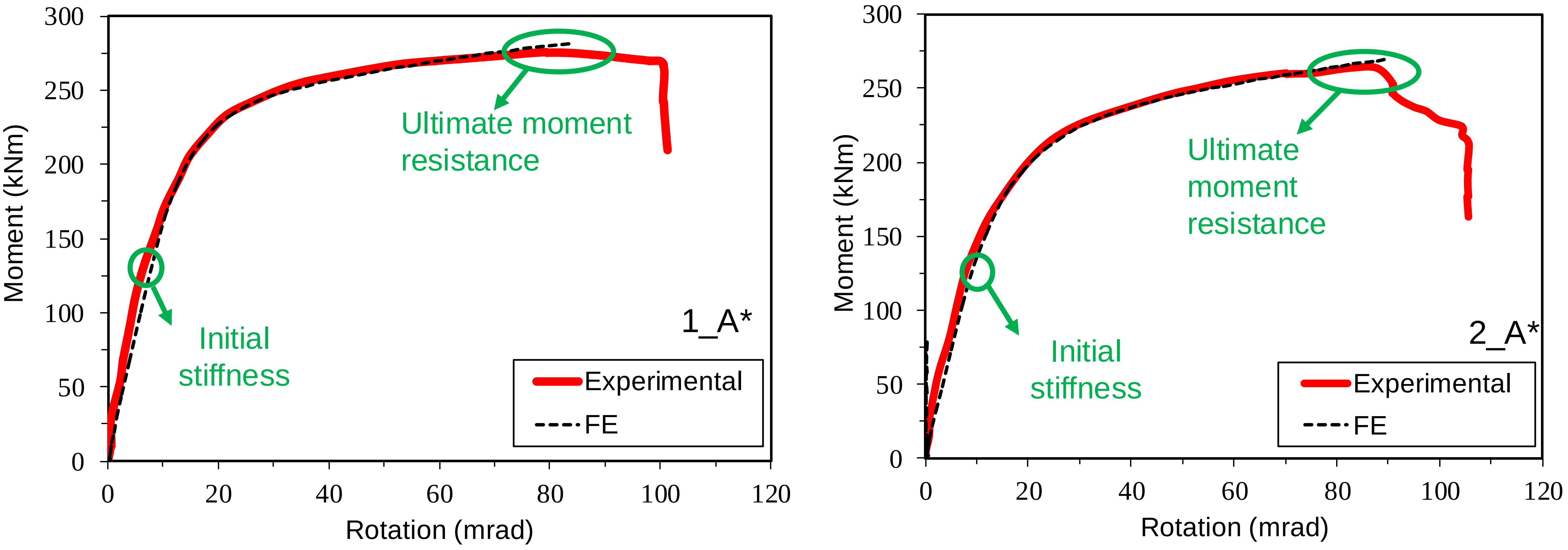

*A: Ambient temperature

Figure 7: Ambient temperature validation moment – rotation curves

Post-fire validation (after exposure to 550 °C)

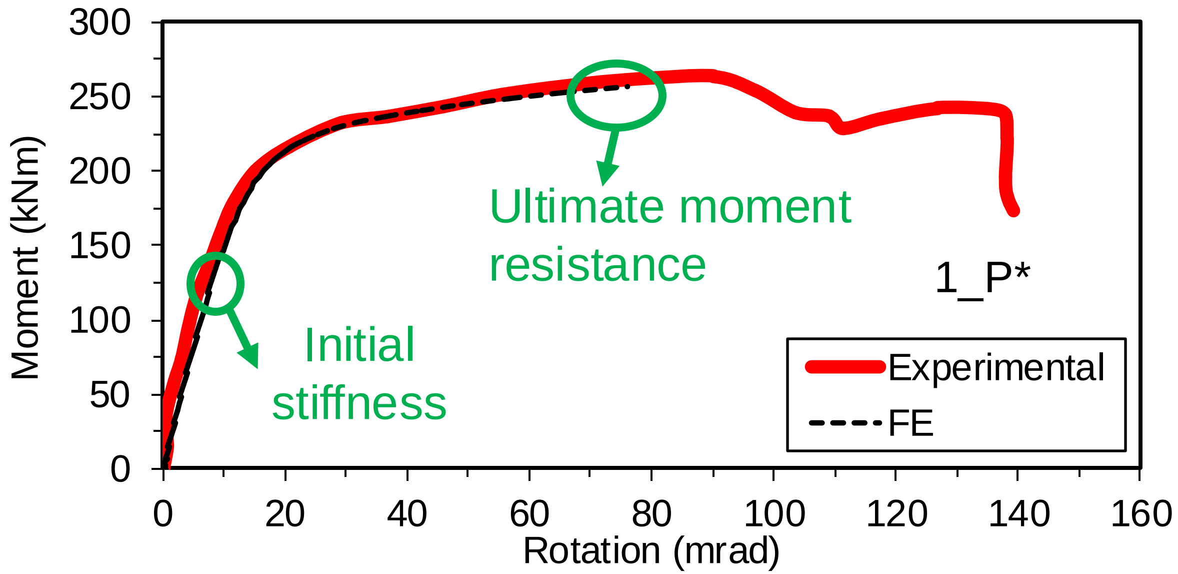

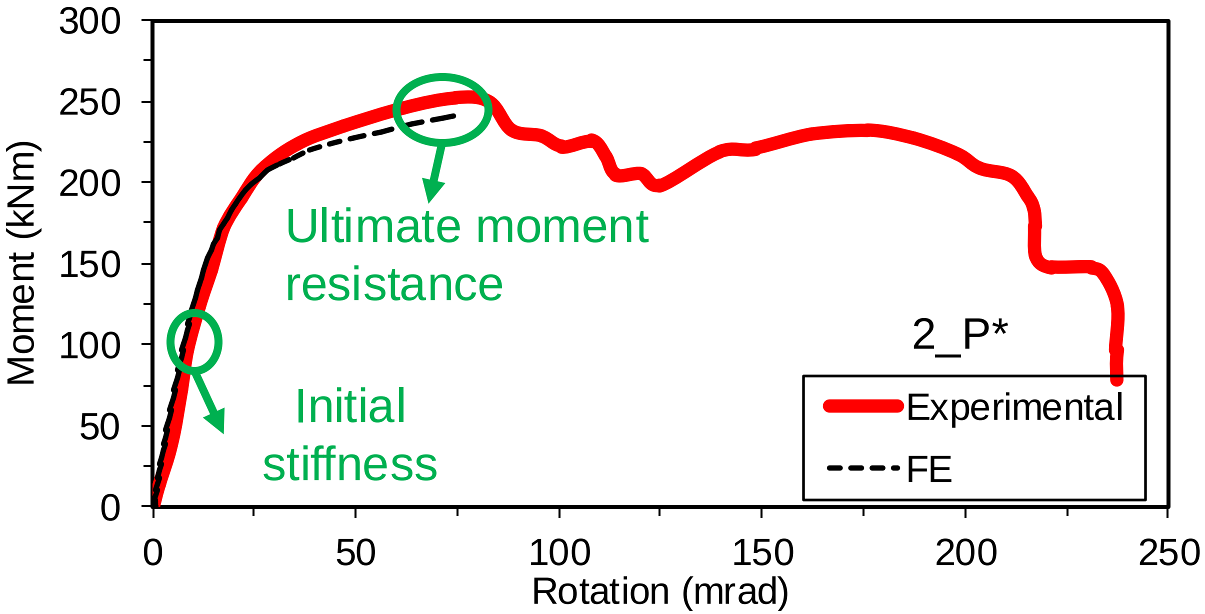

Figure 8: Post-fire validation moment – rotation curves

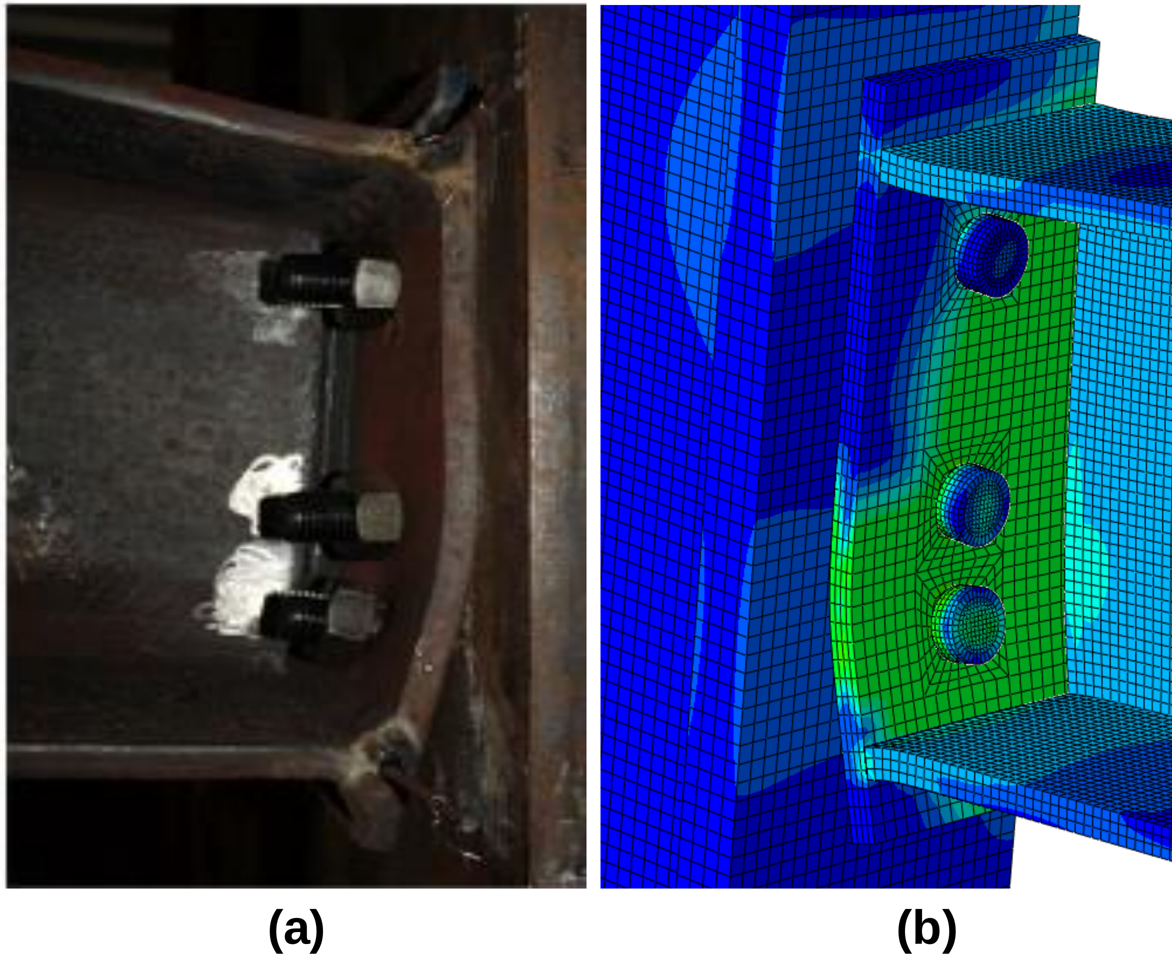

Figure 9: 1_P (a) Experimental [3] (b) FE

*P: Post-fire (after exposure to 550 °C)

Elevated temperature validation (550 °C)

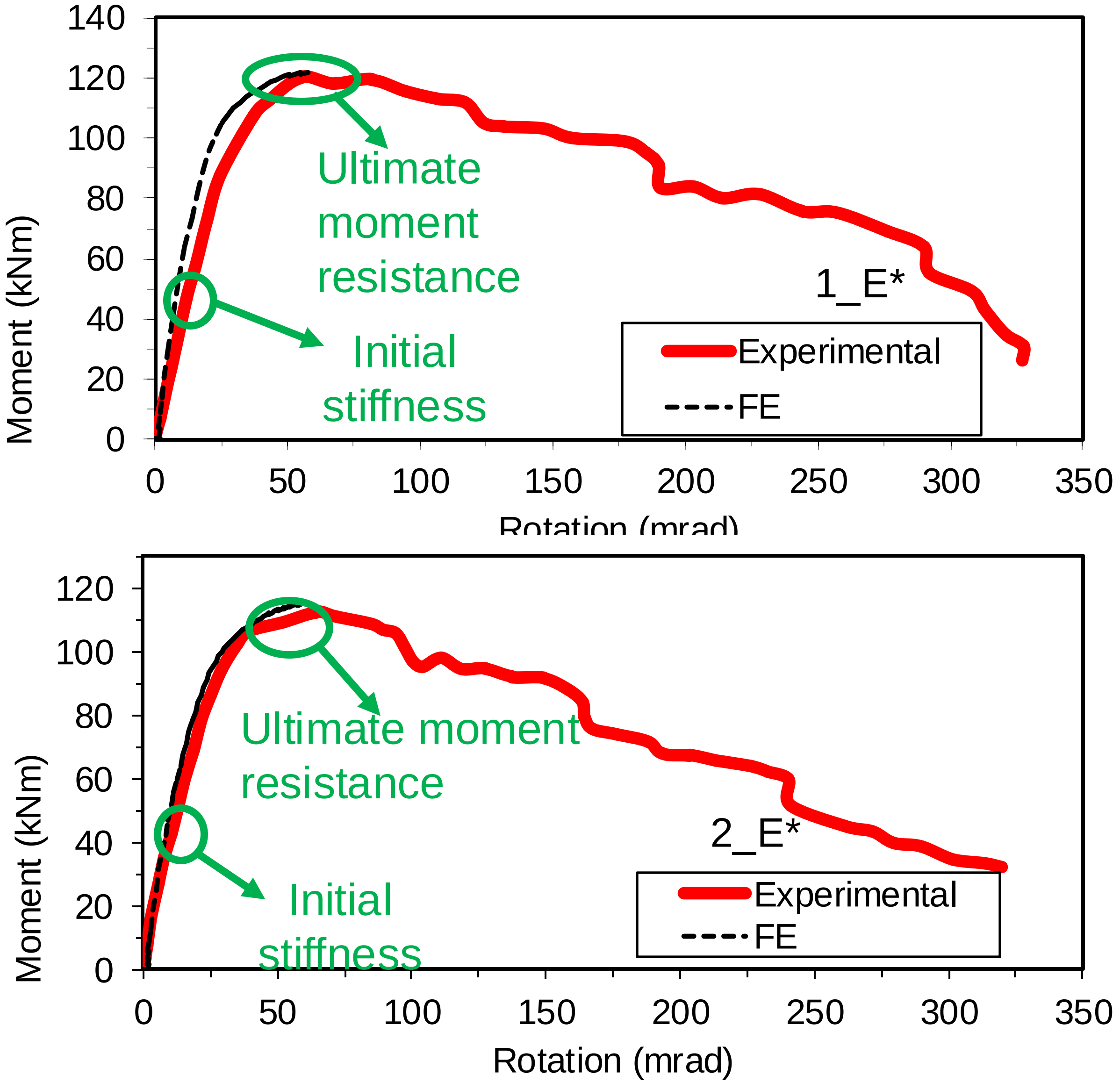

Figure 10: Elevated temperature moment – rotation curves

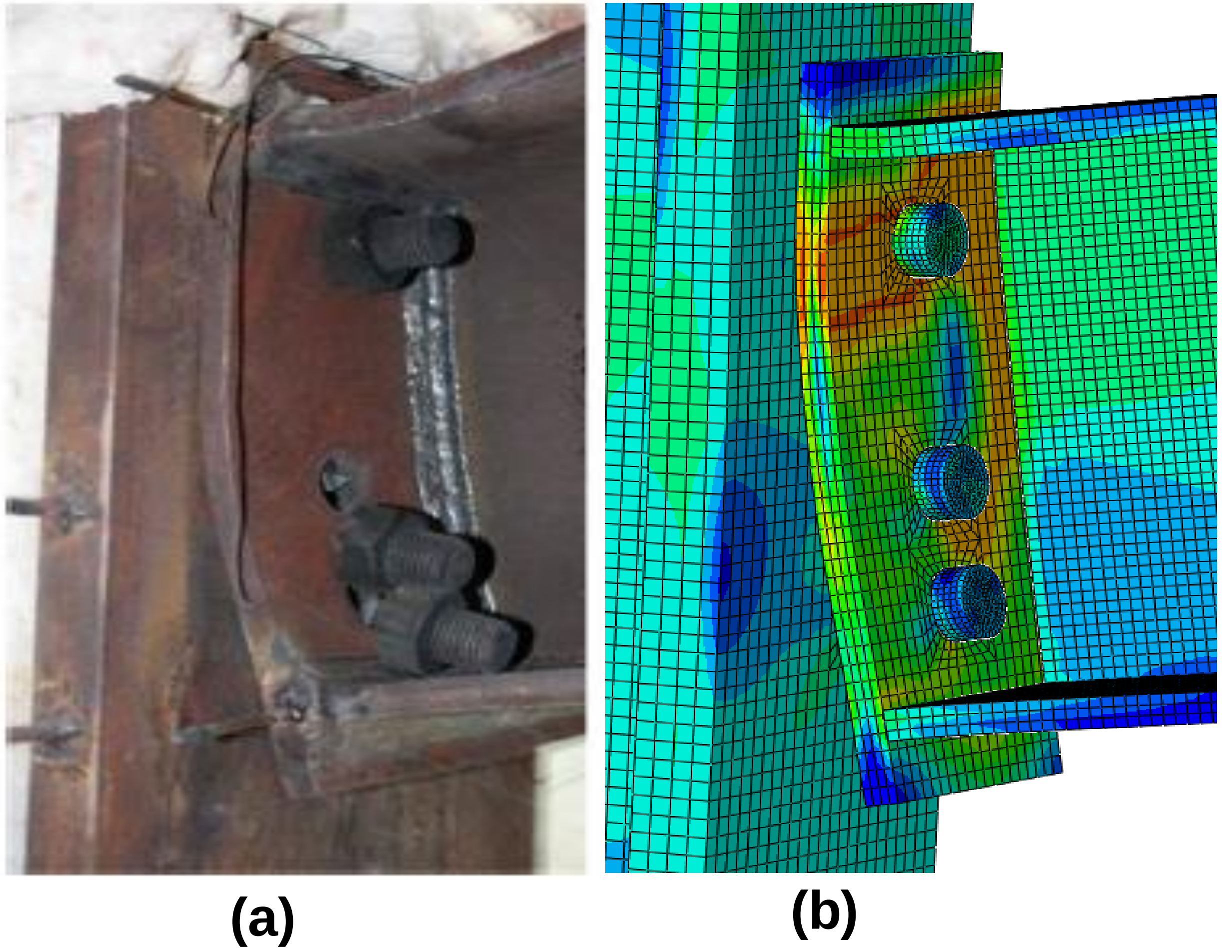

Figure 11: 1_E (a) Experimental [3] (b) FE

*E: Elevated temperature (exposure to 550 °C)

Validation summary

- Maximum deviation of 3.2%
- FE model is accurate at predicting the behaviour of flush endplate connections at ambient, post-fire and elevated temperatures.

Table 2: Comparison between $M_{u,exp}$ and $M_{u,FE}$

Connection ID	T [°C]	$M_{u,exp}$ [kNm]	$M_{u,FE}$ [kNm]	$\frac{M_{u,exp}}{M_{u,FE}}$
1_A	20	272.7	281.7	0.97
2_A	20	120.8	121.9	0.99
1_E	550	264.3	269.7	0.98
2_E	550	113.2	115.7	0.98
1_P	550	261.8	259.7	1.01
2_P	550	252.9	250.5	1.01
			Mean	**0.99**
			CoV	**0.015**

3. Replacing components with H500

Ambient temperature before and after exposure to fire

H500 Endplate: Ambient temperature

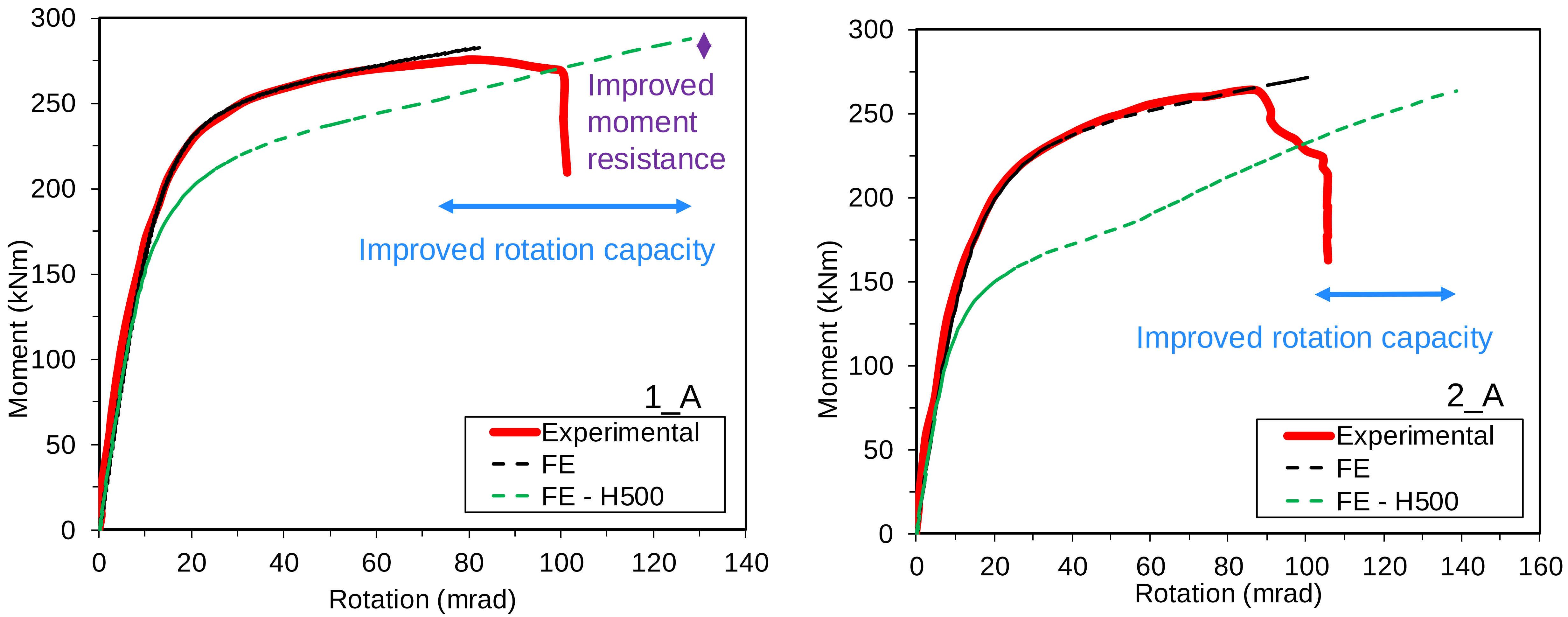

Figure 12: Ambient temperature moment – rotation curves

H500 Endplate: Post-fire (550 °C)

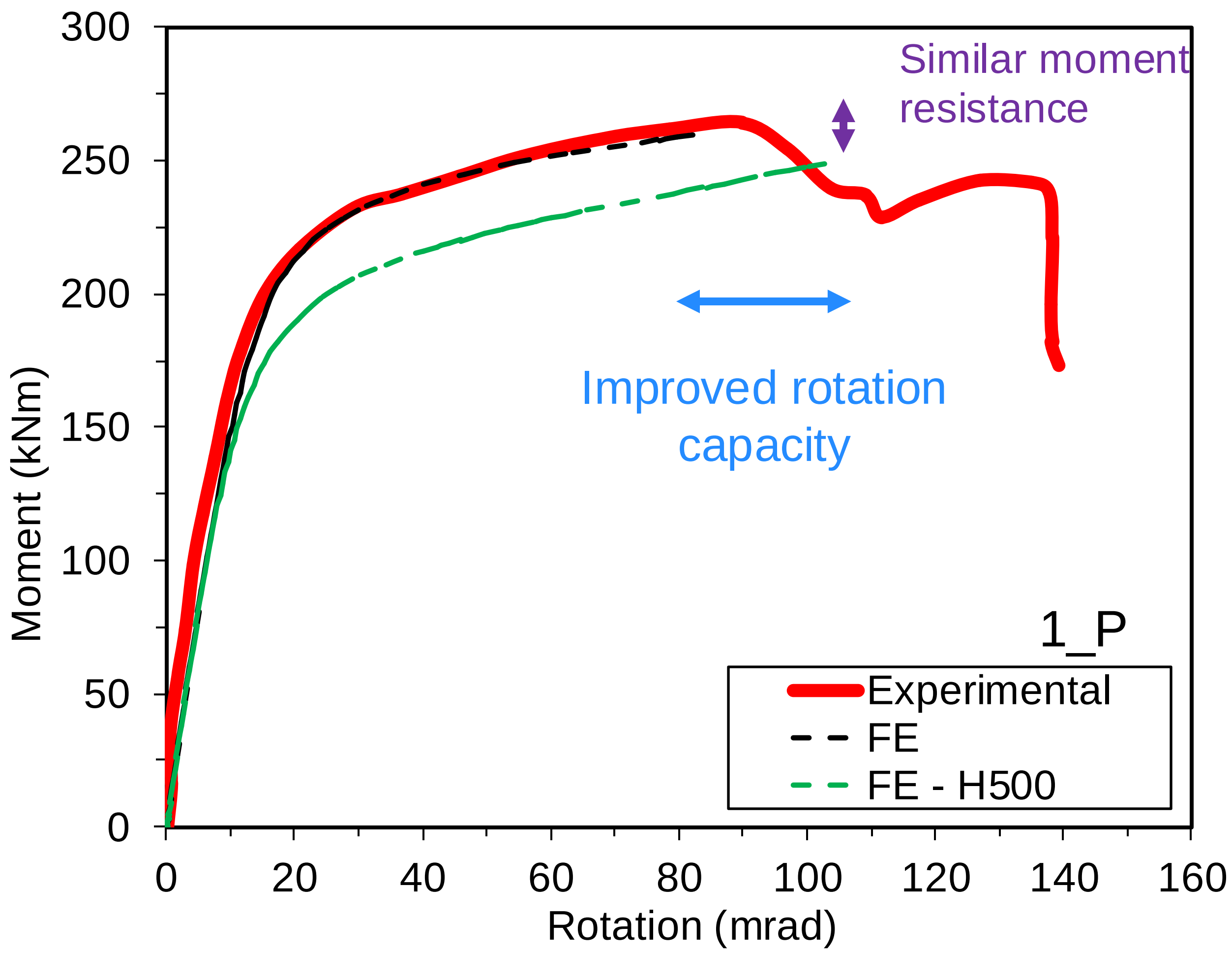

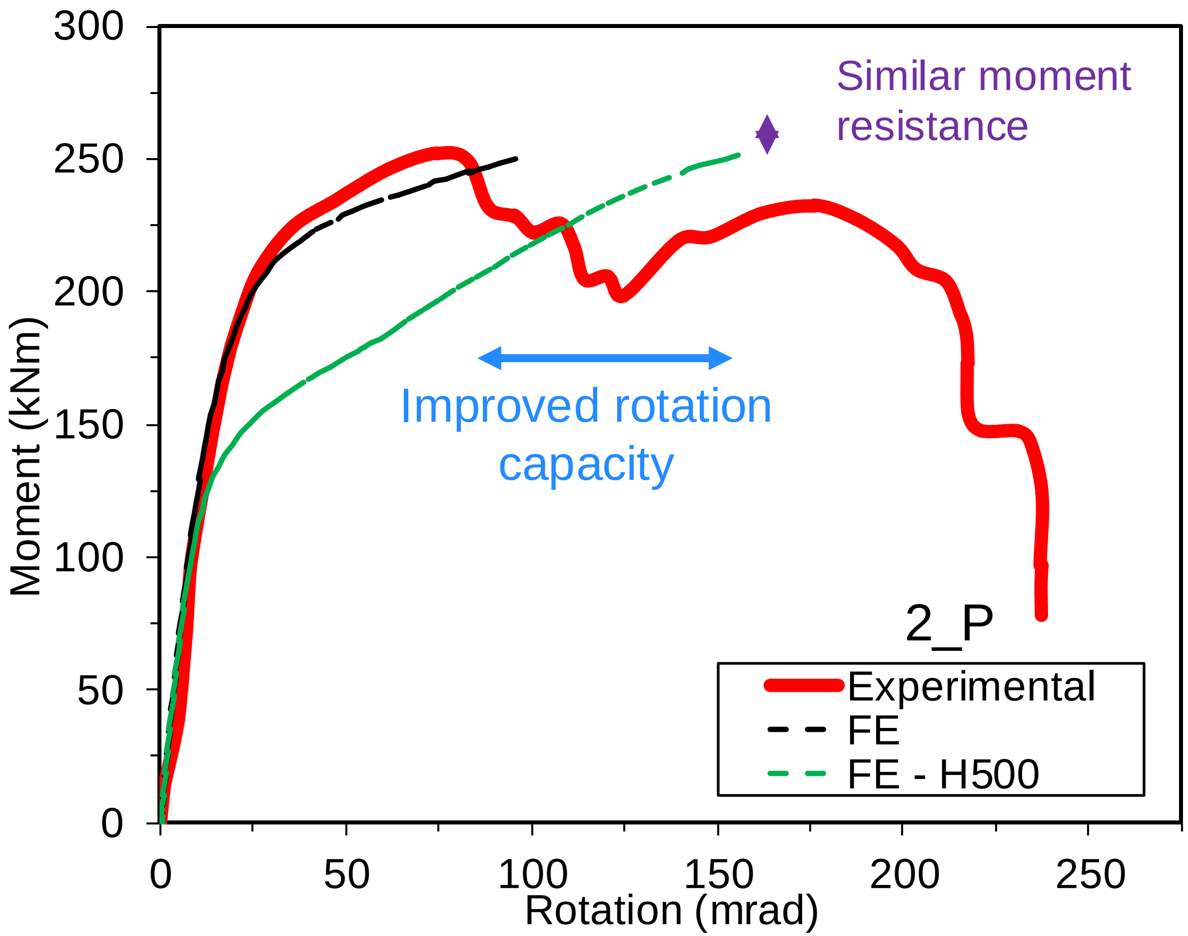

Figure 12: Post-fire temperature moment – rotation curves

During fire

Parametric study with published data

Parametric study

- Connection type 1 used as baseline.
- Beam and column material is Q345 in all studies.

Table 3: Material grades used in the parametric study

Component	Parameters			
Endplate grade	Carbon steel Q345 [3]	High strength steel S690 [3]	Austenitic stainless steel 1.4420 [5]	Ferritic stainless steel 1.4509 [6]
Bolt grade	Grade 8.8 [7]	Grade 10.9 [8]	Grade 12.9 [8]	Austenitic A2-70 [9]
Temperature (°C)	20	300	500	700

- The connections were named in the following format

  "Endplate material – Bolt material – Endplate thickness – Temperature level".

Isothermal fire: Changing endplate grade

T = 20°C   T = 300°C

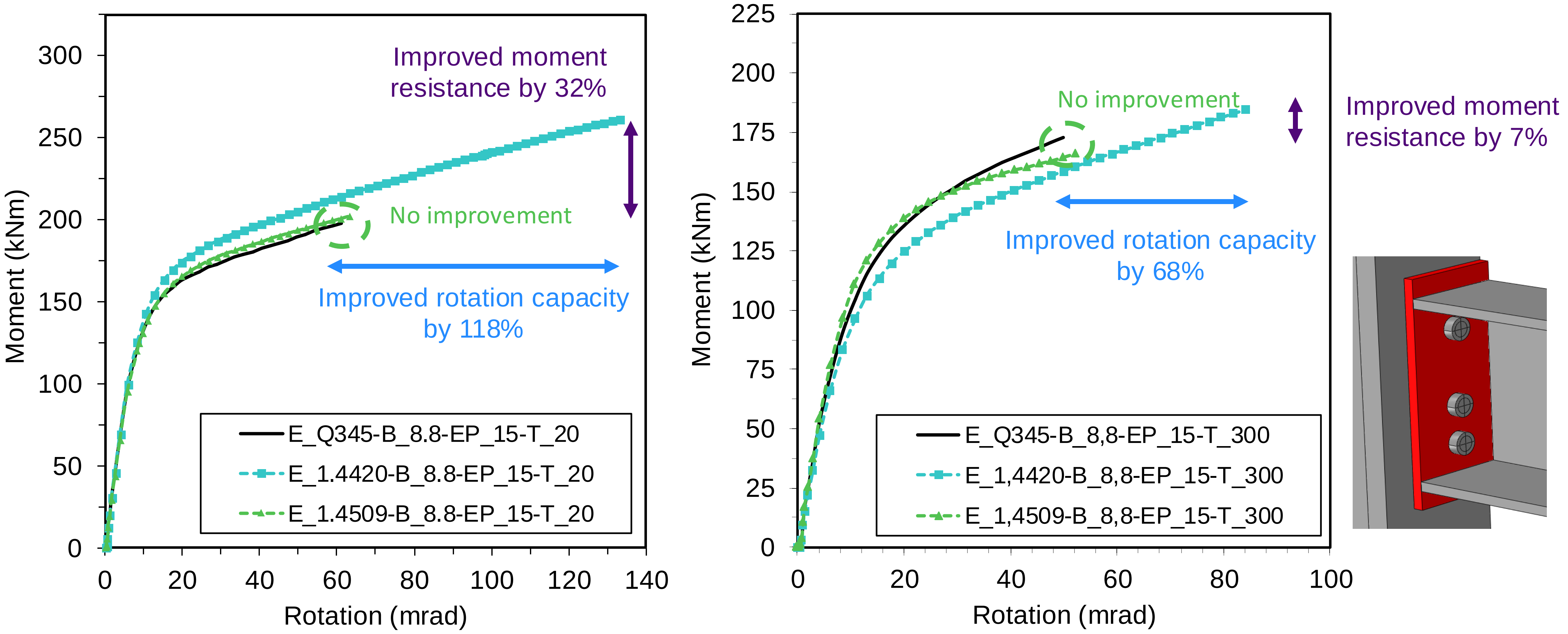

Figure 14: Moment – rotation curves changing endplate grade at ambient and 300°C

Isothermal fire: Changing bolt grade

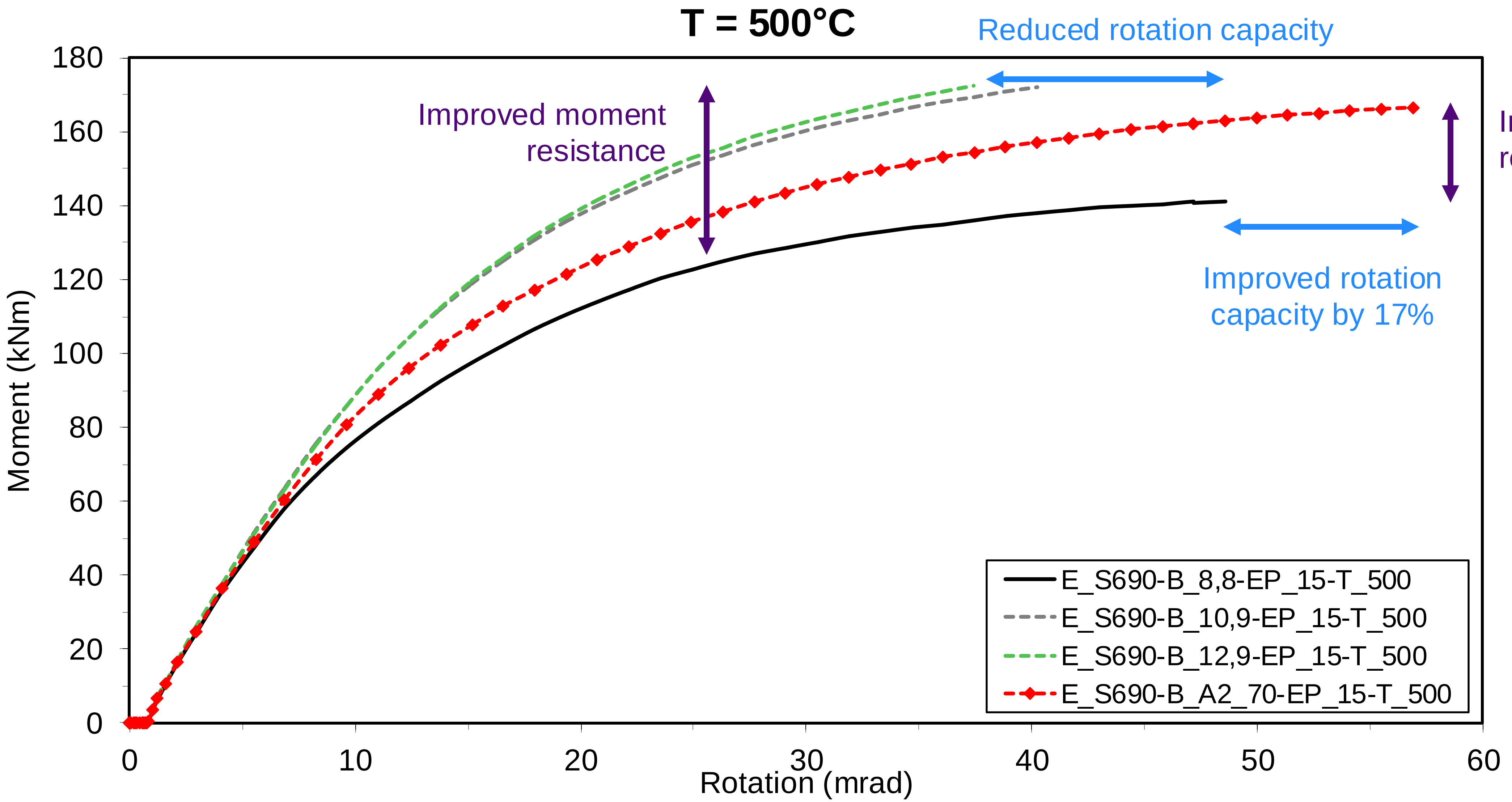

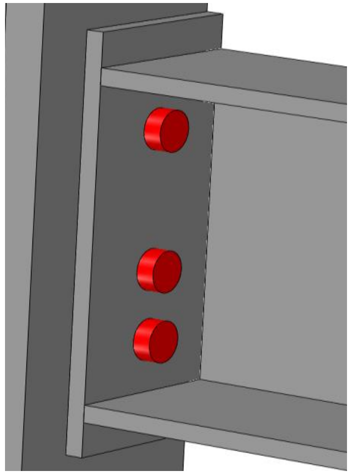

Figure 16: Elevated temperature moment – rotation curves

Isothermal fire: Changing endplate & bolt grade

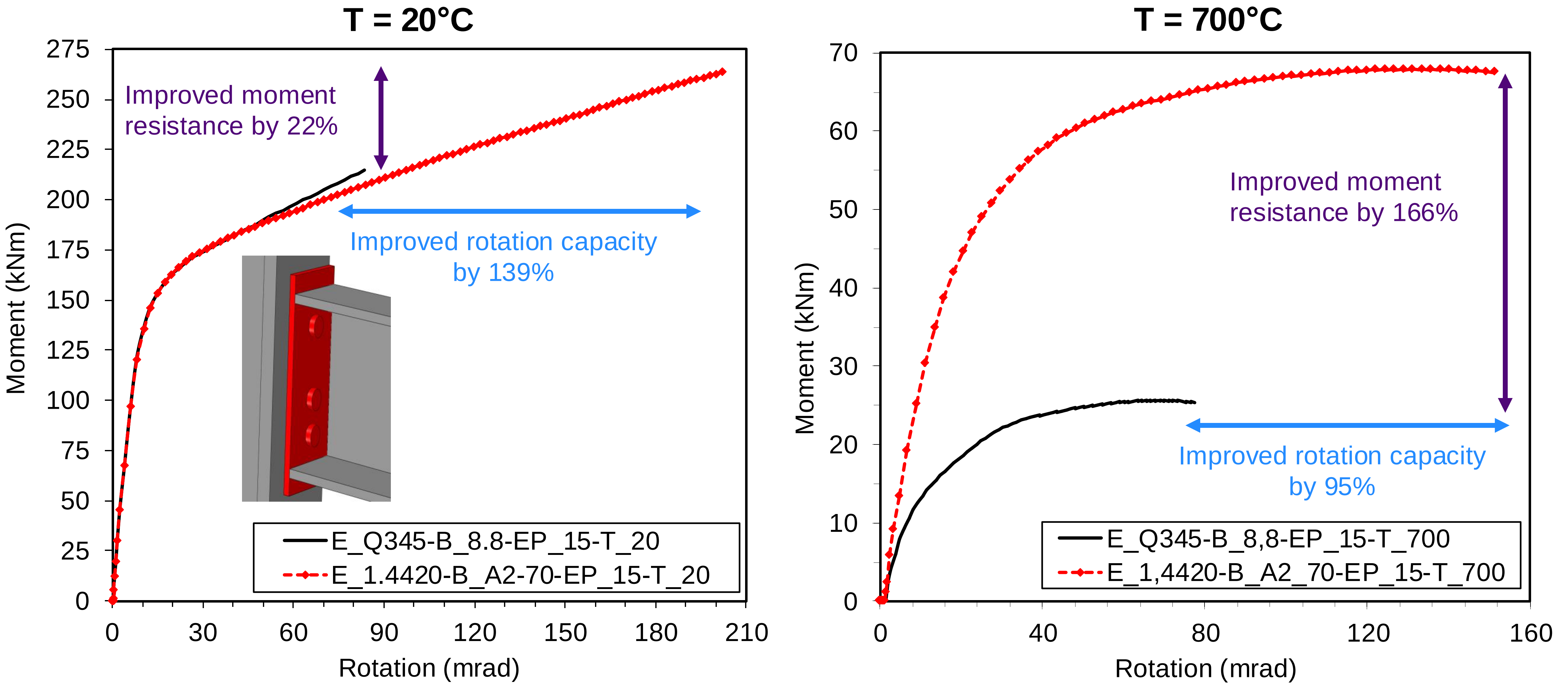

Figure 17: Moment – rotation curves when changing end plate and bolt grade

4. Conclusions

Conclusions and ongoing work

- H500 post-fire tests showed different failure modes after exposure to different temperatures and cooling methods.
- Ultimate moment resistance of H500 compares well with S690 and S960
  - Showing improved rotational capacity at the ultimate moment resistance.
- At elevated temperatures, substituting carbon steel components with stainless steel:
  - Up to 95% increase in rotational capacity
  - Up to 166% increase in ultimate moment resistance

Ongoing work

- Studying metallurgical reasons for brittle failure at 700 – 900 °C using SEM.
- Comparing other grades of stainless steel in parametric study
- Other connection typologies

Thank you for your attention!

Hadi El Samad, **Luke Lapira** and Katherine A. Cashell

hadi.samad.22@ucl.ac.uk, l.lapira@ucl.ac.uk, k.cashell@ucl.ac.uk

Department of Civil, Environmental and Geomatic Engineering, UCL, UK

References

[1] EN 1993-1-2, Design of steel structures - Part 1-2: General rules - Structural fire design, Brussels: CEN, 2004.

[2] Outokumpu. (2019). Ultimate lightweight solutions.

[3] Qiang, X.et al. (2014). Eng. Struct., 64, 23–38. https://doi.org/10.1016/j.engstruct.2014.01.028

[4] B.S. Institution. Structural use of steelwork in building. Part 8: code of practice for fire resistant design; 2003.

[5] Liang, Y. et al. (2019). Journal of Constructional Steel Research, 152, 261–273. https://doi.org/10.1016/j.jcsr.2018.04.028

[6] Manninen, T., & Säynäjäkangas J. (2012). *Mechanical Properties of Ferritic Stainless Steels at Elevated Temperature*.

[7] Saglik, H. et al. (2024). Journal of Structural Engineering, 150(6). https://doi.org/10.1061/jsendh.steng-12629

[8] Pang, X. et al. (2019). *Results in Physics*, *13*. https://doi.org/10.1016/j.rinp.2019.102156

[9] Wang, H. et al. (2021). Engineering Structures, 235. https://doi.org/10.1016/j.engstruct.2021.111973